# High-energy cosmic-ray acceleration

*M. Bustamante*[1]*, G.D. Carrillo Montoya*[2]*, W. de Paula*[3]*, J.A. Duarte Chavez*[4]*, A.M. Gago*[1]*, H. Hakobyan*[5]*, P. Jez*[6]*, J.A. Monroy Montañez*[7]*, A. Ortiz Velasquez*[8]*, F. Padilla Cabal*[9]*, M. Pino Rozas*[10]*, D.J. Rodriguez Patarroyo*[11]*, G.L. Romeo*[12]*, U.J. Saldaña-Salazar*[13]*, M. Velasquez*[14] *and M. von Steinkirch*[15]

[1]Pontificia Universidad Católica del Perú, Lima, Peru
[2] EPFL, Switzerland and U. of Wisconsin, USA
[3] Instituto Tecnológico de Aeronáutica, São Josè dos Campos, Brazil
[4] Universidad Nacional de Colombia - Sede Bogota, Colombia
[5] Universidad Tecnica Federico Santa Maria, Valparaiso, Chile
[6] Niels Bohr Institute, Copenhagen, Denmark
[7] Universidad de los Andes, Bogota, Colombia
[8] Instituto de Ciencias Nucleares, Mexico
[9] InSTEC, La Habana, Cuba
[10]Pontificia Universidad Católica de Chile, Santiago, Chile
[11] Universidad Antonio Narino, Bogota, Colombia
[12] Universidad de Buenos Aires, Argentina
[13] UNAM, Mexico
[14] Universidad de Antioquia, Medellin, Colombia
[15] University of São Paulo, Brazil

**Abstract**

We briefly review the basics of ultrahigh-energy cosmic-ray acceleration. The Hillas criterion is introduced as a geometrical criterion that must be fulfilled by potential acceleration sites, and energy losses are taken into account in order to obtain a more realistic scenario. The different available acceleration mechanisms are presented, with special emphasis on Fermi shock acceleration and its prediction of a power-law cosmic-ray energy spectrum. We conclude that first-order Fermi acceleration, though not entirely satisfactory, is the most promising mechanism for explaining the ultra-high-energy cosmic-ray flux.

A copy of the slides presented during the oral report at the school can be found at the URL below
`http://cern.ch/PhysicSchool/LatAmSchool/2009/Presentations/pDG1.pdf`

## 1 Introduction

In 1912, Victor Hess, using a balloon flight, measured the intensity of the ionizing radiation as a function of altitude. This date represents the begining of the history of cosmic rays. Since then, we have learned about many of their features, such as their large energy span (1–$10^{20}$ eV), their composition (they are made up of protons, nuclei, electrons and other charged particles), and the behaviour, as a function of energy, of their flux.

However, the source and origin of the highest-energy cosmic rays still elude us [1, 2]. There are two general approaches: in top-down scenarios [3], cosmic rays are produced as secondaries of the decay of heavy particles, while in bottom-up scenarios, the energetic cosmic-ray protons and nuclei are accelerated within regions of intense magnetic fields. During recent years, experiments like AGASA [4, 5] and HiRes [6] have been trying to answer these questions. A newly-built experiment, the Pierre Auger Observatory, has performed observations [7] that hint at active galactic nuclei—galaxies with a supermassive central black hole—as sources of the highest-energy cosmic rays. A plot of the differential cosmic-ray energy spectrum, produced with data from several experiments, is shown in Figure 1.

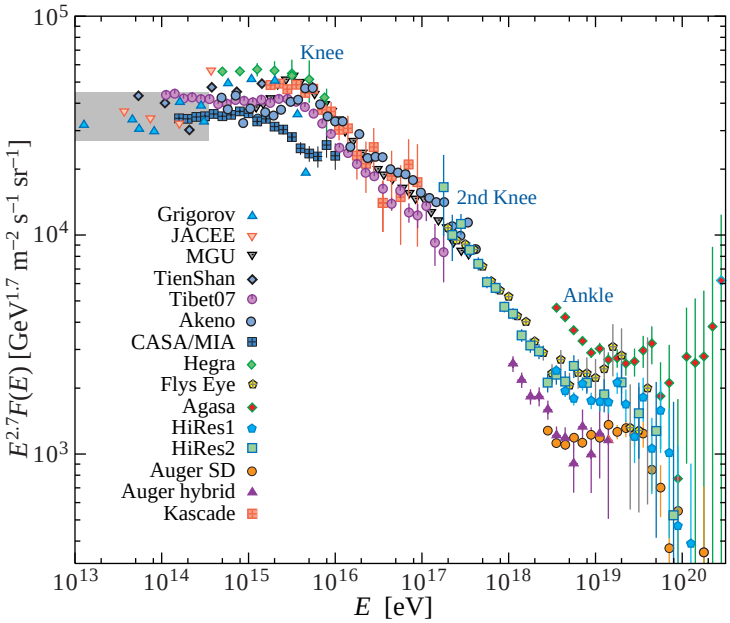


**Fig. 1:** Cosmic-ray differential energy spectrum, reconstructed from air showers observed by various experiments. The grey box is the region where direct observations of cosmic rays have been made. The spectrum has been multiplied by $E^{2.7}$ to enhance the kinks due to changes in the spectral index: the first one near $10^{15} - 10^{16}$ eV (the *knee*), the second one at $10^{17}$ eV (the *second knee*) and the last one around $10^{19}$ eV (the *ankle*). Figure extracted from Ref. [8]

The purpose of this review is to give a brief description of the general constraints on acceleration sites, as well as of the first- and second-order Fermi acceleration mechanism. For a more in-depth review of the theory and observation of cosmic rays, the reader can consult, for example, Refs. [9, 10].

## 2 General constraints on acceleration sites

In order to be considered as a possible source of ultra-high-energy cosmic rays (UHECRs), an astrophysical object has to fulfil several conditions [11]:

- **geometry**: the accelerated particle should be maintained within the object during the acceleration process;
- **power**: the source should be able to provide the necessary energy for the accelerated particles;
- **radiation losses**: within the accelerating field the energy gained by a particle should be no less than its radiation energy loss;
- **interaction losses**: the energy lost by a particle due to its interaction with other particles should not be greater than its energy gain;
- **emissivity**: the density and power of sources must be enough to account for the observed UHECR flux;
- **coexisting radiation**: the accompanying photon and neutrino flux, and the low-energy cosmic-ray flux, should not be greater than the observed fluxes (this constraint must be satisfied by the flux from a single source and by the diffuse flux).

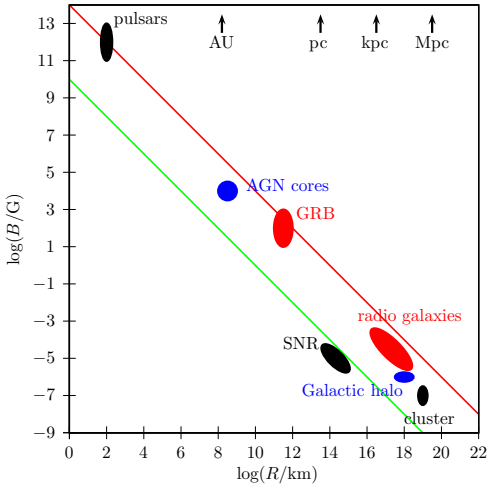


**Fig. 2:** Hillas plot. Sources above the top (red) line are able to accelerate protons up to $10^{21}$ eV, while sources above the bottom (green) line are able to accelerate iron up to $10^{20}$ eV. Figure reproduced from Ref. [12]

### 2.1 The Hillas criterion

If a particle escapes from the region where it was being accelerated, it will be unable to gain more energy. This situation imposes a limit on its maximum energy that can be expressed as follows:

$$\varepsilon_{\max} = qBR\,, \tag{1}$$

where $q$ is the electric charge of the accelerated particle, $B$ is the magnetic field, and $R$ is the size of the accelerator. Equation (1) is obtained by demanding that the Larmor radius of the particle, $R_L = \varepsilon/(qB)$, not exceed the size of the acceleration region. This is a general geometrical criterion known as the *Hillas criterion*, and is useful in selecting potential acceleration sites.

Figure 2 is an example of a Hillas plot which, for a given maximum energy $\varepsilon_{\max}$ of the accelerated particle, shows the relation between the source's magnetic field strength $B$ and its size $R$. Sources above the top line are able to accelerate protons up to $10^{21}$ eV, while sources above the bottom line are able to accelerate iron up to $10^{20}$ eV.

A more realistic description of particle acceleration takes into account the energy lost during the process. The maximum energy that a particle can obtain in an accelerator if energy losses are accounted for is given by the solution of $d\varepsilon^{(+)}/dt = d\varepsilon^{(-)}/dt$, i.e., the situation where energy lost and gained is equal. The maximum energy of the particle is hence given by the minimum between the value obtained from this equality and the one obtained from the Hillas criterion. Hillas plots for proton and iron taking into account energy losses are shown in Figure 3.

UHECRs are believed to have both a galactic (for energies below the knee) [13] and an extragalactic (above the knee) component [14]. Some potential galactic sources include type II supernovae, pulsars and shock acceleration in supernova remnants, while extragalactic ones include active galaxies and gamma-ray bursts.

## 3 General forms of acceleration

### 3.1 Inductive acceleration mechanism

This mechanism is also called *one-shot acceleration* and occurs when a particle is accelerated in a continuous way by an ordered field [see Figure 4(a)]. Radiation losses from accelerated charged particles moving at relativistic velocities are composed of two terms [11], attributed to synchrotron and curvature radiation.

#### *3.1.1 One-shot acceleration with synchrotron-dominated losses*

In this regime the maximum energy is given by

$$\varepsilon_s = \sqrt{\frac{3}{2}} \frac{m^2}{q^{3/2}} B^{-1/2} \, , \tag{2}$$

where $B$ is the strength of the magnetic field, and $m$, $q$ are the mass and charge of the particle, respectively. This notation will be valid for the sections below.

#### *3.1.2 One-shot acceleration with curvature-dominated losses*

In the special case when $\overrightarrow{\mathbf{v}} // \overrightarrow{\mathbf{E}} // \overrightarrow{\mathbf{B}}$, curvature losses dominate. This might be the situation in the vicinity of neutron stars and black holes. The corresponding maximum energy is

$$\varepsilon_c = \frac{3}{2}^{1/4} \frac{m}{q^{1/4}} B^{1/4} R^{1/2} \, . \tag{3}$$

### 3.2 Diffusive acceleration

In this mechanism the particle is accelerated in bursts, as a result of its interaction with regions of high magnetic field intensity, as shown in Figure 4(b). The maximum energy, considering synchrotron-dominated losses, is [11]

$$\varepsilon_d \simeq \frac{3}{2} \frac{m^4}{q^4} B^{-2} R^{-1} \, . \tag{4}$$

Diffusive acceleration, and in particular Fermi acceleration (see next Section) is the preferred acceleration mechanism in bottom-up scenarios of cosmic-ray production.

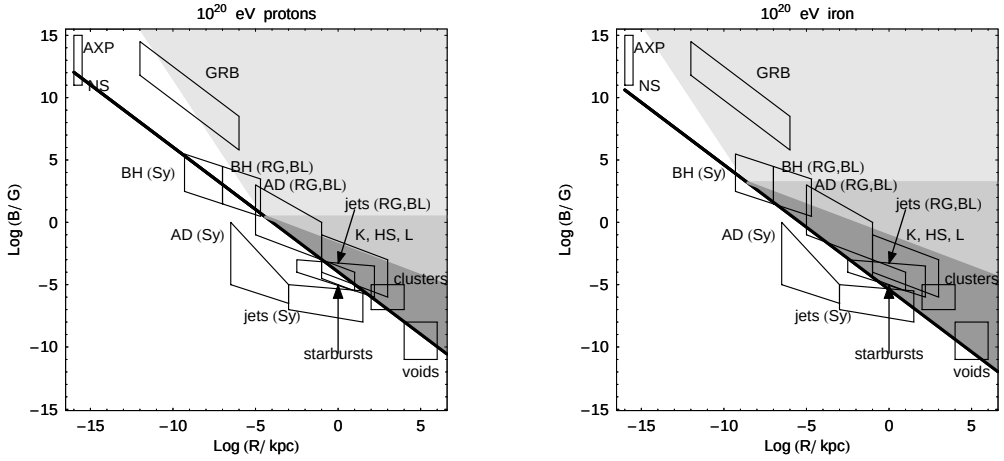


(a) (b)

**Fig. 3: (a)** Hillas plot for $10^{20}$ eV protons, including energy losses. The thick line is the lower boundary due to the Hillas criterion. The light grey region is allowed by one-shot acceleration with curvature-dominated losses, the grey region is allowed by one-shot acceleration with synchrotron-dominated losses, and the dark grey region is allowed by both one-shot and diffusive acceleration. **(b)** Same plot for $10^{20}$ eV iron nuclei. Figures reproduced from Ref. [11]

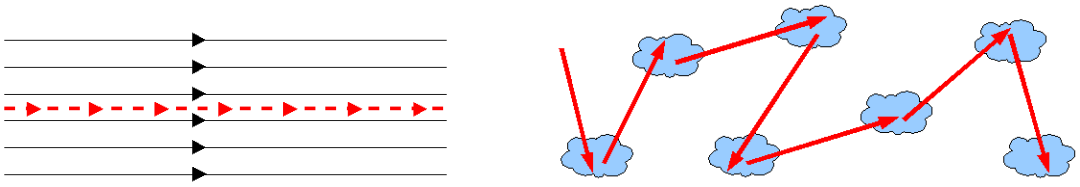

(a) (b)

**Fig. 4: (a)** One-shot acceleration. **(b)** Diffusive shock acceleration

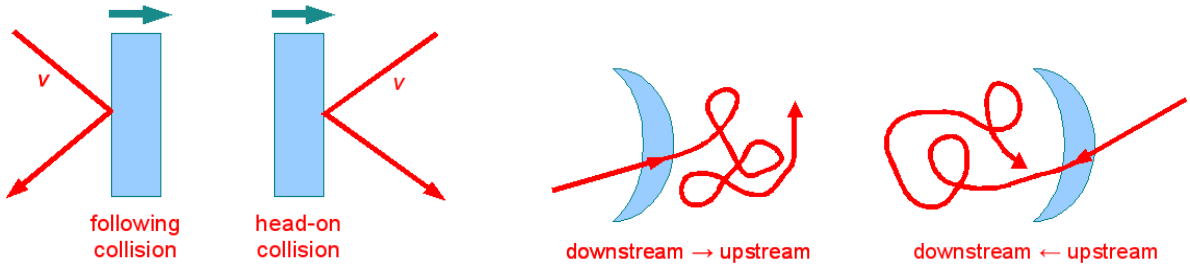


(a) (b)

**Fig. 5: (a)** Second-order Fermi acceleration. **(b)** First-order Fermi acceleration.

## 4 Fermi acceleration

### 4.1 Second-order Fermi acceleration

This first version of the Fermi acceleration mechanism (later dubbed *second-order acceleration*) was proposed by Enrico Fermi in 1949 [15] and explains the acceleration of relativistic particles by means of their collision with interstellar clouds. These clouds move randomly and act as 'magnetic mirrors', so that the particles are reflected off them, as shown in Figure 5(a).

After some calculations [12, 16] it can be shown that the average energy gain per collision is

$$\left\langle \frac{\Delta E}{E} \right\rangle = \frac{8}{3} \left( \frac{v}{c} \right)^2 , \tag{5}$$

where $v$ and $c$ are the speed of the cloud and of the particle, respectively. The average energy gain is proportional to $(v/c)^2$: the process is known as "second-order" acceleration owing to the value of the exponent. If we calculate the average time between collisions, an energy rate can be derived from Equation (5):

$$\frac{dE}{dt} = \frac{4}{3} \left( \frac{v^2}{cL} \right) E = \alpha E, \tag{6}$$

where $L$ is the mean free path between clouds, along the field lines. It is possible to find the energy spectrum $N(E)$ by solving a diffusion-loss equation in the steady state and considering this energy rate, plus the assumption that $\tau_{\text{esc}}$ is the characteristic time for a particle to remain in the accelerating region. In so doing, one finds that

$$N(E)\, dE = \text{const.} \times E^{1+\frac{1}{\alpha \tau_{\text{esc}}}}\, dE\ . \tag{7}$$

Even though second-order acceleration succeeds in generating a power-law spectrum, it is not a completely satisfactory mechanism. First, on account of the observed low cloud density, the energy gain is very slow. Second, the mechanism fails to explain the observed value of 2.7 for the exponent in the power-law spectrum: the value of the exponent is determined by the uncertain value of the combination $\alpha \tau_{\text{esc}}$.

### 4.2 First-order Fermi acceleration

Before we discuss first-order Fermi acceleration it is convenient to formulate the Fermi mechanism in a more general and simple way, valid for both the second- and first-order versions. For that purpose, we define the average energy of the particle after one collision as $E = \beta E_0$, with $E_0$ the energy before the collision, and $P$ as the probability that the particle remains, after one collision, inside the acceleration region. After $n$ collisions, we have $N = N_0 P^n$ particles with energies $E = E_0 \beta^n$. Hence the energy spectrum results in

$$N(E)dE = \text{const.} \times E^{-1+\frac{\ln P}{\ln \beta}}\, dE\,. \tag{8}$$

It is clear that in this approach, which exhibits the expected power law, the parameters $P$ and $\beta$ can be translated into the ones that were found for the Fermi second-order mechanism, and are also going to be applied to the first-order one.

The goal of the first-order acceleration mechanism is to obtain an energy gain that is linear in $(v/c)$, a condition that would make the acceleration process more effective, especially at relatively high values of $v$. This set-up will occur when the relativistic particles collide with strong shock waves (e.g., like those produced in supernova explosions, active galactic nuclei, etc.), which can reach supersonic velocities ($10^3$ times the velocity of an interstellar cloud).

Owing to the turbulence behind the shock and the irregularities in front of it, the particle velocity distribution is isotropic in the frames of reference where the interstellar gas is at rest on either side of the shock. Consequently, there is a complete symmetry when a high-energy particle crosses the shock from downstream to upstream or from upstream to downstream; this is illustrated in Figure 5(b).

In both types of crossing, the particle gains energy. It is possible to show [16] that in a round trip the average energy gain is given by

$$\left\langle \frac{\Delta E}{E} \right\rangle = \frac{4}{3}\left(\frac{v}{c}\right)\,. \tag{9}$$

Another quantity that must be considered is the particle escape probability $P_{\text{esc}}$ (equivalent to $1 - P$) from the shock. Using kinetic theory, one obtains

$$P_{\text{esc}} = \frac{4}{3}\left(\frac{v}{c}\right). \tag{10}$$

Replacing these two parameters in Equation (8), we get

$$N\,(E)\,dE = \text{const.} \times E^{-2}\,dE\,. \tag{11}$$

In spite of not having obtained the observed exponent of 2.7 yet, the first-order mechanism is very promising, being the most effective and probable one, since shock waves are expected to be present in different astrophysical enviroments. In addition, in contrast to the second-order mechanism, here we find a fixed numerical value for the exponent.

## 5 Summary

We have presented a brief review of the mechanisms that could accelerate particles up to high energies ($10^{20}$ eV) at galactic and extragalactic astrophysical sites. These mechanisms must fulfil a series of general requirementes, which include geometrical and energetical constraints. Among these, the Hillas criterion, a geometrical constraint on the size of the acceleration region, is most useful in selecting potential sources of cosmic rays. We have also presented two general forms of acceleration: one-shot acceleration, which requires ordered magnetic fields, and diffusive acceleration, in which particles gain energy by bouncing off random magnetic clouds. The latter type of acceleration includes Fermi shock acceleration, which correctly predicts a power-law cosmic-ray energy spectrum, albeit with a different exponent than the one that has been measured. Of the two versions of the Fermi mechanism, the first-order seems to be the most promising one to explain the ultra-high-energy cosmic-ray flux, even though it does not manage to predict the observed spectral index.

## Acknowledgements

The authors would like to thank the organizers of the 5th CERN Latin American School of High-Energy Physics.

## References

[1] R. Diehl, [arXiv:astro-ph/0902.4795].

[2] M. Ostrowski, Astropart. Phys. **18** (2002) 229 [arXiv:astro-ph/0101053].

[3] N. Busca, D. Hooper, and E. W. Kolb, Phys. Rev. D **73** (2006) 123001 [arXiv:astro-ph/0603055].

[4] G. I. Rubtsov *et al.*, Phys. Rev. D **73** (2006) 063009 [arXiv:astro-ph/0601449].

[5] K. Shinozaki [AGASA Collaboration], Nucl. Phys. Proc. Suppl. **151** (2006) 3.

[6] D. R. Bergman [HiRes Collaboration], [arXiv:astro-ph/0807.2814].

[7] J. Abraham *et al.* [Pierre Auger Collaboration], Astropart. Phys. **29** (2008) 188 [Erratum ibid. **30** (2008) 45] [arXiv:astro-ph/0712.2843].

[8] C. Amsler *et al.* [Particle Data Group], Phys. Lett. B **667** (2008) 1.

[9] J. W. Cronin, Rev. Mod. Phys. **71** (1999) S165.

[10] M. Nagano and A. A. Watson, Rev. Mod. Phys. **72** (2000) 689.

[11] K. Ptitsyna and S. Troitsky, [arXiv:astro-ph/0808.0367].

[12] M. Kachelriess, [arXiv:astro-ph/0801.4376].

[13] S. Gabici, [arXiv:astro-ph/0811.0836].

[14] L. Anchordoqui, H. Goldberg, S. Reucroft, and J. Swain, Phys. Rev. D **64** (2001) 123004 [arXiv:hep-ph/0107287].

[15] E. Fermi, Phys. Rev. **75** (1949) 1169.

[16] M. S. Longair, High Energy Astrophysics, Vol. 2: Stars, the Galaxy and the Interstellar Medium (Cambridge University Press, 2008).